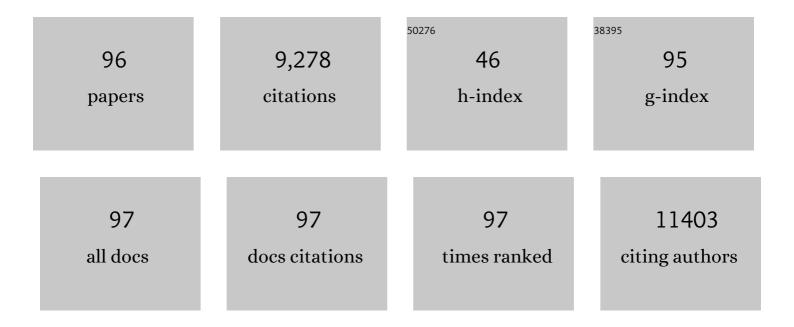
## Stephen V Kershaw

List of Publications by Year in descending order

Source: https://exaly.com/author-pdf/7376244/publications.pdf Version: 2024-02-01



#	Article	IF	CITATIONS
1	Lead Halide Perovskite Nanocrystals in the Research Spotlight: Stability and Defect Tolerance. ACS Energy Letters, 2017, 2, 2071-2083.	17.4	888
2	Control of Emission Color of High Quantum Yield CH <sub>3</sub> NH <sub>3</sub> PbBr <sub>3</sub> Perovskite Quantum Dots by Precipitation Temperature. Advanced Science, 2015, 2, 1500194.	11.2	536
3	Color-Switchable Electroluminescence of Carbon Dot Light-Emitting Diodes. ACS Nano, 2013, 7, 11234-11241.	14.6	471
4	Zn-Alloyed CsPbl <sub>3</sub> Nanocrystals for Highly Efficient Perovskite Light-Emitting Devices. Nano Letters, 2019, 19, 1552-1559.	9.1	395
5	Infrared-Emitting Colloidal Nanocrystals: Synthesis, Assembly, Spectroscopy, and Applications. Small, 2007, 3, 536-557.	10.0	385
6	Narrow bandgap colloidal metal chalcogenide quantum dots: synthetic methods, heterostructures, assemblies, electronic and infrared optical properties. Chemical Society Reviews, 2013, 42, 3033.	38.1	374
7	Aqueous Based Semiconductor Nanocrystals. Chemical Reviews, 2016, 116, 10623-10730.	47.7	364
8	Thickness-Dependent Full-Color Emission Tunability in a Flexible Carbon Dot Ionogel. Journal of Physical Chemistry Letters, 2014, 5, 1412-1420.	4.6	361
9	Trifluoroacetate induced small-grained CsPbBr3 perovskite films result in efficient and stable light-emitting devices. Nature Communications, 2019, 10, 665.	12.8	350
10	Colloidally Prepared HgTe Nanocrystals with Strong Room-Temperature Infrared Luminescence. Advanced Materials, 1999, 11, 552-555.	21.0	312
11	Thermally Stable Copper(II)-Doped Cesium Lead Halide Perovskite Quantum Dots with Strong Blue Emission. Journal of Physical Chemistry Letters, 2019, 10, 943-952.	4.6	274
12	Smoothing the energy transfer pathway in quasi-2D perovskite films using methanesulfonate leads to highly efficient light-emitting devices. Nature Communications, 2021, 12, 1246.	12.8	274
13	Growth mechanism of strongly emitting CH3NH3PbBr3 perovskite nanocrystals with a tunable bandgap. Nature Communications, 2017, 8, 996.	12.8	210
14	Improved Stability and Photodetector Performance of CsPbl <sub>3</sub> Perovskite Quantum Dots by Ligand Exchange with Aminoethanethiol. Advanced Functional Materials, 2019, 29, 1902446.	14.9	206
15	25th Anniversary Article: Ion Exchange in Colloidal Nanocrystals. Advanced Materials, 2013, 25, 6923-6944.	21.0	170
16	Bright Orange Electroluminescence from Lead-Free Two-Dimensional Perovskites. ACS Energy Letters, 2019, 4, 242-248.	17.4	166
17	Magnetically Engineered Semiconductor Quantum Dots as Multimodal Imaging Probes. Advanced Materials, 2014, 26, 6367-6386.	21.0	145
18	Hydrogen Peroxide Assisted Synthesis of Highly Luminescent Sulfur Quantum Dots. Angewandte Chemie - International Edition, 2019, 58, 7040-7044.	13.8	137

STEPHEN V KERSHAW

#	Article	IF	CITATIONS
19	Bright CsPbl <sub>3</sub> Perovskite Quantum Dot Light-Emitting Diodes with Top-Emitting Structure and a Low Efficiency Roll-Off Realized by Applying Zirconium Acetylacetonate Surface Modification. Nano Letters, 2020, 20, 2829-2836.	9.1	137
20	Ruthenium(II) Complex Incorporated UiO-67 Metal–Organic Framework Nanoparticles for Enhanced Two-Photon Fluorescence Imaging and Photodynamic Cancer Therapy. ACS Applied Materials & Interfaces, 2017, 9, 5699-5708.	8.0	129
21	Photocurrent Enhancement of HgTe Quantum Dot Photodiodes by Plasmonic Gold Nanorod Structures. ACS Nano, 2014, 8, 8208-8216.	14.6	116
22	Advances in metal halide perovskite nanocrystals: Synthetic strategies, growth mechanisms, and optoelectronic applications. Materials Today, 2020, 32, 204-221.	14.2	114
23	Hydrothermal synthesis of hierarchical SnO <sub>2</sub> microspheres for gas sensing and lithium-ion batteries applications: Fluoride-mediated formation of solid and hollow structures. Journal of Materials Chemistry, 2012, 22, 2140-2148.	6.7	112
24	Mercury Telluride Quantum Dot Based Phototransistor Enabling High-Sensitivity Room-Temperature Photodetection at 2000 nm. ACS Nano, 2017, 11, 5614-5622.	14.6	110
25	Revealing the Formation Mechanism of CsPbBr <sub>3</sub> Perovskite Nanocrystals Produced via a Slowedâ€Down Microwaveâ€Assisted Synthesis. Angewandte Chemie - International Edition, 2018, 57, 5833-5837.	13.8	109
26	Temperature-Dependent Exciton and Trap-Related Photoluminescence of CdTe Quantum Dots Embedded in a NaCl Matrix: Implication in Thermometry. Small, 2016, 12, 466-476.	10.0	107
27	Polyhedral Oligomeric Silsesquioxane Enhances the Brightness of Perovskite Nanocrystal-Based Green Light-Emitting Devices. Journal of Physical Chemistry Letters, 2016, 7, 4398-4404.	4.6	105
28	Cesium Lead Chloride/Bromide Perovskite Quantum Dots with Strong Blue Emission Realized via a Nitrate-Induced Selective Surface Defect Elimination Process. Journal of Physical Chemistry Letters, 2019, 10, 90-96.	4.6	103
29	Using Polar Alcohols for the Direct Synthesis of Cesium Lead Halide Perovskite Nanorods with Anisotropic Emission. ACS Nano, 2019, 13, 8237-8245.	14.6	84
30	Fast, Airâ€Stable Infrared Photodetectors based on Sprayâ€Deposited Aqueous HgTe Quantum Dots. Advanced Functional Materials, 2014, 24, 53-59.	14.9	82
31	Insight into Strain Effects on Band Alignment Shifts, Carrier Localization and Recombination Kinetics in CdTe/CdS Core/Shell Quantum Dots. Journal of the American Chemical Society, 2015, 137, 2073-2084.	13.7	81
32	Highly Integrated Supercapacitor‣ensor Systems via Material and Geometry Design. Small, 2016, 12, 3393-3399.	10.0	78
33	Materials aspects of semiconductor nanocrystals for optoelectronic applications. Materials Horizons, 2017, 4, 155-205.	12.2	78
34	CsPbI <sub>3</sub> /PbSe Heterostructured Nanocrystals for High-Efficiency Solar Cells. ACS Energy Letters, 2020, 5, 2401-2410.	17.4	77
35	Spontaneous Selfâ€Assembly of Cesium Lead Halide Perovskite Nanoplatelets into Cuboid Crystals with High Intensity Blue Emission. Advanced Science, 2019, 6, 1900462.	11.2	69
36	Organic nanostructures of thermally activated delayed fluorescent emitters with enhanced intersystem crossing as novel metal-free photosensitizers. Chemical Communications, 2016, 52, 11744-11747.	4.1	68

STEPHEN V KERSHAW

#	Article	IF	CITATIONS
37	Multidentate Ligand Polyethylenimine Enables Bright Color-Saturated Blue Light-Emitting Diodes Based on CsPbBr <sub>3</sub> Nanoplatelets. ACS Energy Letters, 2021, 6, 477-484.	17.4	65
38	In Situ Fabrication of Flexible, Thermally Stable, Large-Area, Strongly Luminescent Copper Nanocluster/Polymer Composite Films. Chemistry of Materials, 2017, 29, 10206-10211.	6.7	58
39	Ligandâ€Controlled Formation and Photoluminescence Properties of CH <sub>3</sub> NH <sub>3</sub> PbBr <sub>3</sub> Nanocubes and Nanowires. ChemNanoMat, 2017, 3, 303-310.	2.8	57
40	Shuttling Photoelectrochemical Electron Transport in Tricomponent CdS/rGO/TiO <sub>2</sub> Nanocomposites. Journal of Physical Chemistry C, 2013, 117, 20406-20414.	3.1	55
41	In Situ versus ex Situ Assembly of Aqueous-Based Thioacid Capped CdSe Nanocrystals within Mesoporous TiO <sub>2</sub> Films for Quantum Dot Sensitized Solar Cells. Journal of Physical Chemistry C, 2012, 116, 484-489.	3.1	52
42	Solution Processed Hybrid Polymer: HgTe Quantum Dot Phototransistor with High Sensitivity and Fast Infrared Response up to 2400Ânm at Room Temperature. Advanced Science, 2020, 7, 2000068.	11.2	52
43	Cdâ€Rich Alloyed CsPb <sub>1â€</sub> <i><sub>x</sub></i> Cd <i><sub>x</sub></i> Br <sub>3</sub> Perovskite Nanorods with Tunable Blue Emission and Fermi Levels Fabricated through Crystal Phase Engineering. Advanced Science, 2020, 7, 2000930.	11.2	52
44	Solution-Processed Ambipolar Organic Thin-Film Transistors by Blending p- and n-Type Semiconductors: Solid Solution versus Microphase Separation. ACS Applied Materials & Interfaces, 2015, 7, 28019-28026.	8.0	51
45	A Nearâ€Infrared Absorbing and Emissive Quadruple Helicene Enabled by the Scholl Reaction of Perylene. Angewandte Chemie - International Edition, 2022, 61, .	13.8	50
46	Reversible transformation between CsPbBr <sub>3</sub> and Cs <sub>4</sub> PbBr <sub>6</sub> nanocrystals. CrystEngComm, 2018, 20, 4900-4904.	2.6	48
47	Stretchable and Thermally Stable Dual Emission Composite Films of On-Purpose Aggregated Copper Nanoclusters in Carboxylated Polyurethane for Remote White Light-Emitting Devices. ACS Applied Materials & Interfaces, 2016, 8, 33993-33998.	8.0	47
48	Mesoporous Aluminum Hydroxide Synthesized by a Singleâ€Source Precursorâ€Decomposition Approach as a Highâ€Quantumâ€Yield Blue Phosphor for UVâ€Pumped Whiteâ€Lightâ€Emitting Diodes. Advanced Materia 2017, 29, 1604284.	ls21.0	47
49	Impact of D <sub>2</sub> O/H <sub>2</sub> O Solvent Exchange on the Emission of HgTe and CdTe Quantum Dots: Polaron and Energy Transfer Effects. ACS Nano, 2016, 10, 4301-4311.	14.6	43
50	Amine-Terminated Carbon Dots Linking Hole Transport Layer and Vertically Oriented Quasi-2D Perovskites through Hydrogen Bonds Enable Efficient LEDs. ACS Nano, 2022, 16, 9679-9690.	14.6	41
51	Au@HgxCd1-xTe core@shell nanorods by sequential aqueous cation exchange for near-infrared photodetectors. Nano Energy, 2019, 57, 57-65.	16.0	38
52	Cd <sub><i>x</i></sub> Hg <sub>(1â^'<i>x</i>)</sub> Te Alloy Colloidal Quantum Dots: Tuning Optical Properties from the Visible to Nearâ€Infrared by Ion Exchange. Particle and Particle Systems Characterization, 2013, 30, 346-354.	2.3	36
53	Integrated Plasmonic Infrared Photodetector Based on Colloidal HgTe Quantum Dots. Advanced Materials Technologies, 2019, 4, 1900354.	5.8	36
54	Morphology Control of Luminescent Carbon Nanomaterials: From Dots to Rolls and Belts. ACS Nano, 2021, 15, 1579-1586.	14.6	35

STEPHEN V KERSHAW

#	Article	IF	CITATIONS
55	Carbon Dots Detect Water-to-Ice Phase Transition and Act as Alcohol Sensors <i>via</i> Fluorescence Turn-Off/On Mechanism. ACS Nano, 2021, 15, 6582-6593.	14.6	34
56	Chemically Synthesized Carbon Nanorods with Dual Polarized Emission. ACS Nano, 2019, 13, 12024-12031.	14.6	31
57	Bright, Magnetic NIR-II Quantum Dot Probe for Sensitive Dual-Modality Imaging and Intensive Combination Therapy of Cancer. ACS Nano, 2022, 16, 8076-8094.	14.6	31
58	Hydrogen Peroxide Assisted Synthesis of Highly Luminescent Sulfur Quantum Dots. Angewandte Chemie, 2019, 131, 7114-7118.	2.0	29
59	Highly luminescent covalently bonded layered double hydroxide–fluorescent dye nanohybrids. Journal of Materials Chemistry C, 2014, 2, 4490-4494.	5.5	27
60	Room Temperature Synthesis of HgTe Quantum Dots in an Aprotic Solvent Realizing High Photoluminescence Quantum Yields in the Infrared. Chemistry of Materials, 2017, 29, 7859-7867.	6.7	27
61	Investigation of the Exchange Kinetics and Surface Recovery of Cd <sub><i>x</i></sub> Hg <sub>1–<i>x</i></sub> Te Quantum Dots during Cation Exchange Using a Microfluidic Flow Reactor. Chemistry of Materials, 2017, 29, 2756-2768.	6.7	26
62	Infrared Emitting HgTe Quantum Dots and Their Waveguide and Optoelectronic Devices. Zeitschrift Fur Physikalische Chemie, 2015, 229, 23-64.	2.8	24
63	Carrier Multiplication Mechanisms and Competing Processes in Colloidal Semiconductor Nanostructures. Materials, 2017, 10, 1095.	2.9	24
64	Oxalic Acid Enabled Emission Enhancement and Continuous Extraction of Chloride from Cesium Lead Chloride/Bromide Perovskite Nanocrystals. Small, 2019, 15, e1901828.	10.0	24
65	Strongly Luminescent Dion–Jacobson Tin Bromide Perovskite Microcrystals Induced by Molecular Proton Donors Chloroform and Dichloromethane. Advanced Functional Materials, 2021, 31, 2102182.	14.9	24
66	Co-Doping of Cerium and Bismuth into Lead-Free Double Perovskite Cs <sub>2</sub> AgInCl <sub>6</sub> Nanocrystals Results in Improved Photoluminescence Efficiency. ACS Nanoscience Au, 2022, 2, 93-101.	4.8	24
67	Multiple exciton generation in cluster-free alloy Cd <sub>x</sub> Hg <sub>1â^'x</sub> Te colloidal quantum dots synthesized in water. Physical Chemistry Chemical Physics, 2014, 16, 25710-25722.	2.8	22
68	A Building Brick Principle to Create Transparent Composite Films with Multicolor Emission and Selfâ€Healing Function. Small, 2018, 14, e1800315.	10.0	21
69	Broad-Band Photodetectors Based on Copper Indium Diselenide Quantum Dots in a Methylammonium Lead Iodide Perovskite Matrix. ACS Applied Materials & Interfaces, 2020, 12, 35201-35210.	8.0	21
70	Synthesis and Optical Properties of Cubic Chalcopyrite/Hexagonal Wurtzite Core/Shell Copper Indium Sulfide Nanocrystals. Journal of the American Chemical Society, 2019, 141, 20516-20524.	13.7	17
71	Development of Synthetic Methods to Grow Long-Wavelength Infrared-Emitting HgTe Quantum Dots in Dimethylformamide. Chemistry of Materials, 2020, 32, 3930-3943.	6.7	17
72	Narrowing the Photoluminescence of Aqueous CdTe Quantum Dots via Ostwald Ripening Suppression Realized by Programmed Dropwise Precursor Addition. Journal of Physical Chemistry C, 2018, 122, 11109-11118.	3.1	16

#	Article	IF	CITATIONS
73	Phase-Controlled Growth of CuInS <sub>2</sub> Shells to Realize Colloidal CuInSe <sub>2</sub> /CuInS <sub>2</sub> Core/Shell Nanostructures. ACS Nano, 2020, 14, 11799-11808.	14.6	16
74	Growth of Multinary Copper-Based Sulfide Shells on CuInSe <sub>2</sub> Nanocrystals for Significant Improvement of Their Near-Infrared Emission. Chemistry of Materials, 2020, 32, 7842-7849.	6.7	15
75	Bright and Stable Dion-Jacobson Tin Bromide Perovskite Microcrystals Realized by Primary Alcohol Dopants. Chemistry of Materials, 2021, 33, 5413-5421.	6.7	15
76	Fluorinated Euâ€Đoped SnO <sub>2</sub> Nanostructures with Simultaneous Phase and Shape Control and Improved Photoluminescence. Particle and Particle Systems Characterization, 2013, 30, 332-337.	2.3	13
77	Temperature-Controlled Fragmentation and Ripening: Synthesis of ZnSe Nanorods with Variable Dimensions and Crystal Structure Starting from Ultrathin ZnSe Nanowires. Chemistry of Materials, 2020, 32, 3960-3969.	6.7	13
78	Nearâ€Infraredâ€Emitting Cd <sub><i>x</i></sub> Hg <sub>1â^'<i>x</i></sub> Se Nanorods Fabricated by Ion Exchange in an Aqueous Medium. ChemPhysChem, 2013, 14, 2853-2858.	2.1	12
79	Revealing the Formation Mechanism of CsPbBr <sub>3</sub> Perovskite Nanocrystals Produced via a Slowedâ€Down Microwaveâ€Assisted Synthesis. Angewandte Chemie, 2018, 130, 5935-5939.	2.0	12
80	Synthesis of Anisotropic ZnSe Nanorods with Zinc Blende Crystal Structure. Angewandte Chemie - International Edition, 2020, 59, 5385-5391.	13.8	12
81	Two-Dimensional and Subnanometer-Thin Quasi-Copper-Sulfide Semiconductor Formed upon Copper–Copper Bonding. ACS Nano, 2021, 15, 873-883.	14.6	12
82	Phase-Dependent Shell Growth and Optical Properties of ZnSe/ZnS Core/Shell Nanorods. Chemistry of Materials, 2021, 33, 3413-3427.	6.7	12
83	Monodisperse CuInS <sub>2</sub> /CdS and CuInZnS <sub>2</sub> /CdS Core–Shell Nanorods with a Strong Nearâ€Infrared Emission. Advanced Optical Materials, 2022, 10, .	7.3	11
84	Room Temperature Fabrication of Stable, Strongly Luminescent Dion–Jacobson Tin Bromide Perovskite Microcrystals Achieved through Use of Primary Alcohols. Nanomaterials, 2021, 11, 2738.	4.1	9
85	Effects of Repetitive Pressure on the Photoluminescence of Bare and ZnS-Capped CuInS <sub>2</sub> Quantum Dots: Implications for Nanoscale Stress Sensors. ACS Applied Nano Materials, 2022, 5, 5617-5624.	5.0	9
86	Continuous Flow Synthesis of Persistent Luminescent Chromium-Doped Zinc Gallate Nanoparticles. Journal of Physical Chemistry Letters, 2021, 12, 7067-7075.	4.6	8
87	Induction of Wurtzite to Zinc-Blende Phase Transformation in ZnSe Nanorods During Cu(I) Cation Exchange. Chemistry of Materials, 2021, 33, 2398-2407.	6.7	7
88	Proton Transferâ€Driven Modification of 3D Hybrid Perovskites to Form Oriented 2D Ruddlesden–Popper Phases. Small Science, 2022, 2, .	9.9	6
89	Integrated near-infrared photodetector based on colloidal HgTe quantum dot loaded plasmonic waveguide. , 2017, , .		4
90	Enhancement of the Fluorescence Quantum Yield of Thiol-Stabilized CdTe Quantum Dots Through Surface Passivation with Sodium Chloride and Bicarbonate. Zeitschrift Fur Physikalische Chemie, 2018, 232, 1399-1412.	2.8	4

#	Article	IF	CITATIONS
91	Nanothermometry: Temperature-Dependent Exciton and Trap-Related Photoluminescence of CdTe Quantum Dots Embedded in a NaCl Matrix: Implication in Thermometry (Small 4/2016). Small, 2016, 12, 548-548.	10.0	2
92	Shape-Controlled Synthesis of Copper Indium Sulfide Nanostructures: Flowers, Platelets and Spheres. Nanomaterials, 2019, 9, 1779.	4.1	2
93	Synthesis of Anisotropic ZnSe Nanorods with Zinc Blende Crystal Structure. Angewandte Chemie, 2020, 132, 5423-5429.	2.0	2
94	Correction to Temperature Controlled Fragmentation and Ripening: Synthesis of ZnSe Nanorods with Variable Dimensions and Crystal Structure Starting from Ultrathin ZnSe Nanowires. Chemistry of Materials, 2021, 33, 4247-4247.	6.7	1
95	Highly Luminescent and Stable 2D/3D Octadecylammonium/Formamidinium Lead Bromide Perovskite Films. Journal of Physical Chemistry C, 2021, 125, 17501-17508.	3.1	1
96	Polarization Sensitive Plasmonic Photodetector Based on HgTe Quantum Dots. , 2018, , .		0